Interplay of entropic and memory effects in diffusion of methane in silicalite zeolites

Floralba López,[1,2] Rafael Pérez,[1,3] Fernando Ruette,[4] and Ernesto Medina[1,3,*]

[1]*Centro de Física, Instituto Venezolano de Investigaciones Científicas. IVIC, Apartado 21827, Caracas 1020 A, Venezuela*

[2]*Grupo de Química Teórica: Quimico-física de Fluidos y Fenómenos Interfaciales (QUIFFIS), Departamento de Química, Facultad de Ciencias, Universidad de Los Andes, Mérida, Venezuela*

[3]*Departamento de Física, Facultad de Ciencias, Universidad Central de Venezuela, Caracas, Distrito Federal, Venezuela*

[4]*Centro de Química, Instituto Venezolano de Investigaciones Científicas. IVIC, Apartado 21827, Caracas 1020 A, Venezuela*

(Received 4 June 2005; revised manuscript received 17 October 2005; published 27 December 2005)

The role of entropic effects in methane distribution and transport in silicalite zeolites is studied using molecular dynamics in the limit of infinite dilution or small loading. Diffusive behavior and its anisotropy is assessed as a function of temperature where we find both an Arrhenius regime above 250 K and deviations thereof below such temperature. Using a previous probabilistic model, geometrical correlations or memory effects are evidenced and are shown to be enhanced as temperature is reduced. Deviations from Arrhenius behavior are concomitant with entropic effects. We find that, the preference of methane towards presence at intersections or channel centers changes at a threshold temperature. A discrete transition is found from a channel-center preferred phase, at low temperatures, versus an intersection preferred phase at high temperatures with evidence of hysteresis effects. Such entropic effects are also reflected, in diffusive transport, as non-Arrhenius-type behavior. A model based on accessible volume as a function of energy agrees with the simulated transition lending new insight into zeolite cavity design.

DOI: 10.1103/PhysRevE.72.061111 PACS number(s): 05.40.−a, 82.75.Jn, 66.30.Ny

I. INTRODUCTION

The role of entropic effects on the distribution of reactants and products of alkane reactions in zeolites and molecular sieves, is an essential element in catalysis design and optimization that is only beginning to be understood. Diffusion is the main transport mechanism of molecules in zeolites. Thus, how it is affected by entropic effects determines many features of the catalytic process. It is generally taken for granted that diffusion obeys an Arrhenius-type temperature dependence determined by activated processes. Nevertheless, recent studies have shown that such a temperature dependence can be nonmonotonic and even be inverse Arrhenius, because of prefactor effects of entropic origin. Recently Schuring *et al.* [1] reported a reduction in the diffusion coefficient of ethane in Linde Type A (LTA) zeolite as temperature increases essentially due to the available space and the rotational degrees of freedom within zeolite cages creating entropic barriers to diffusion.

Understanding the influence of entropic effects on diffusion explains and predicts experimental results regarding selectivity towards products in reaction within microporous material [2]. Schenk *et al.* [3] have reported that entropy plays an important role in selectivity in hydroconversion of hydrocarbons. In that work, the selective production of ramified paraffin's using molecular sieves is attributed to pore diameters of ≈ 0.75 nm such that there is a preference for shorter branched structures that have a better stacking efficiency. Furthermore, when both ramified and linear alkanes are present, separation of such components is achieved on purely diffusive grounds, determining the selectivity and activity of zeolitic sieves [4].

The molecular dynamics (MD) technique has provided a large amount of information on the behavior of many molecules of interest confined in zeolitic structures, especially regarding the characterization of the nature of adsorptive and diffusive processes [5]. Although the technique is strongly demanding on computational resources, it contains all the dynamic information without making assumptions beyond those that are required to fix ensemble properties (temperature, pressure and chemical potential). The dynamic features are an important point here, since correlations in diffusion are revealing of site preferences within the zeolite, dominant jump processes [6] and jump dynamics where memory effects can arise [7]. Although this technique becomes prohibitively cumbersome for long chained molecules, due to the prolonged relaxation times through the confined structure, for smaller molecules such as methane and ethane one is able to benefit amply from the additional information provided by MD within the hundreds of nanosecond range [1].

Here we focus on the simplest possible alkane molecule, methane, within a silicalite zeolite in the dilute limit. A study of the potential profiles of methane within the silicalite porous space reveals that the lowest potential energy regions are within the central domains of the channels. Thus at zero temperature this would be the place to find methane molecules. Nevertheless, relatively energy-costly intersections comprise an additional accessible volume (entropy) once sufficient energy is available. We will see how this simple observation induces a connection between diffusion temperature dependences and entropy or available space effects at a particular energy scale. A kinetic connection is also established determining memory phenomena as manifested by peculiar relations between diffusion coefficients in the different directions.

The paper is organized as follows. In the next section we describe the MD scheme and the model parameters for

*Author to whom correspondence should be addressed.

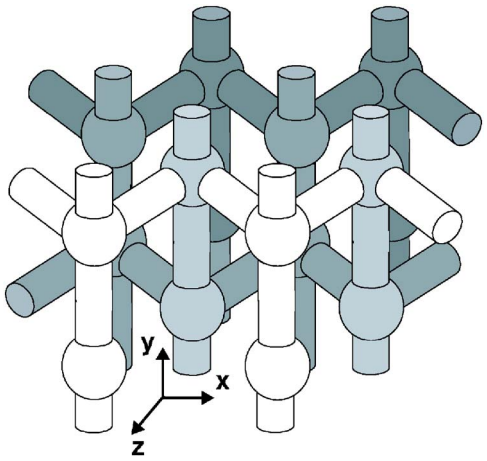

FIG. 1. (Color online) Silicalite structure with the assigned axis convention. Although the drawing is schematic it emphasizes the increased volume at intersections.

methane-zeolite interaction. Only the dilute limit is considered. A simple derivation is given that relates the density per unit length of adsorbate as a function of position, by applying the condition of constant chemical potential throughout the channels of the zeolite. Diffusion within the silicalite is studied, monitoring the three components of the diffusion coefficients to assess anisotropy and memory effects following the theory of Fritzsche and Karger [7]. Non-Arrhenius temperature dependences signal the importance of entropic factors. We address the computation of entropy effects using the expression derived in Sec. III. We obtain a scenario for a change of preference between the channel center and intersections at a particular threshold temperature. The ensuing discussion makes a connection between the interpretation of memory and entropic effects. We end with a summary of our results and the conclusions.

II. MOLECULAR DYNAMICS

Simulation of methane in silicalite was performed using MD. The silicalite host, whose connected structure is depicted schematically in Fig. 1, was modeled with atomic detail, and considered a rigid structure block of two unit cells with total dimensions 20 Å $\times$ 20 Å $\times$ 27 Å, although tests for the size effects of the simulation block were extended up to eight unit cells. The boundary conditions were chosen periodic in three dimensions. The methane units were modeled as a soft sphere in the united atom approximation with a Van der Waals radius of 2 Å. As we consider the dilute limit, interactions are disregarded between the methane molecules. A long discussion has developed in the literature, regarding the effect of making the lattice flexible, that is critically reviewed in Ref. [8]. The possibility of vibrations is indeed the true mechanism (together with sorbate interactions) for thermalization. Recent detailed simulations for methane in silicalite have shown that diffusion is enhanced by a flexible lattice [8,9]. Nevertheless, changes in the diffusion coefficients are very uniform in the three spatial directions and decrease substantially with temperature. The effect of flexible methane molecules, explicitly describing hydrogen, has an even smaller effect. Although such details are not described in our MD we focus not on reproducing accurately known experimental results but on establishing relations between interesting effects such as diffusion, distribution of molecules, and entropic effects within the confines of a porous structure of silicalite.

The interaction between methane and the protruding oxygen sites were assumed to follow a Lennard-Jones potential

$$U_{ij} = \frac{B_{ij}}{r_{ij}^{12}} - \frac{A_{ij}}{r_{ij}^{6}}, \tag{1}$$

between units i and j (methane and oxygen unit on wall), and where the parameters $A_{ij}=2.326\times10^{4}$ KJ $Å^{6}$/mole and $B_{ij}=3.992\times10^{7}$ KJ $Å^{12}$/mole are computed using the Slater-Kirkwood relation [10]. The cutoff distance for this potential was fixed at 10 Å, distance beyond which no appreciable changes occur in the measured variables of the system. The parameters used were tested to reproduce appropriate adsorption energies known from previous MD simulations and experiments [11], and diffusion constants as reported in the literature.

The time step for the simulation was taken to be 1 fs. After an initial run of 10^{7} time steps (10 ns), in order to randomize from the initial configuration (several initial configurations were analyzed), the temperature was set to the desired value using rescaling of velocities [14] and monitoring the temperature drift to determine the rescaling time interval. In order to check whether temperature control affected the diffusion results, microcanonical simulations with a technique similar to that described in Ref. [12] was performed with no appreciable variations to that of rescaling of velocities. The evaluation stage of MD was performed for longer times at lower temperatures, so that one could achieve the same precision in the diffusion coefficient and account for the effects of diffusion slowing down. Below 200 K we gathered data for 10 ns while above such temperature it was enough to record for a 5 ns interval. For the slowest diffusion times τ between intersections $\tau=d^{2}/6D$, where $d\sim10$ Å is the distance between intersections, the evaluation time is at least 10τ.

III. TRANSVERSE ENTROPY

In diffusive equilibrium, achieved when chemical potentials are equalized throughout the channels of a zeolite, one can derive a relation for the number of particles $N(y)$ to be found at a coordinate y along the main channel within a slice Δy (see Fig. 2) starting from the relation

$$\frac{1}{k_B T}\nabla U(y,\rho) = -\nabla \ln n(y,\rho), \tag{2}$$

where k_B is Boltzmann's constant, $n(y,\rho)$ is the density at coordinate y along the main channel, and ρ the radial coordinate perpendicular to y. $U(y,\rho)$ is the potential energy seen by molecules at position (y,ρ) (which assumes cylindrical symmetry) along the channel. Taking the y component of the equation, one can explicitly solve it to find that $n(y,\rho)$

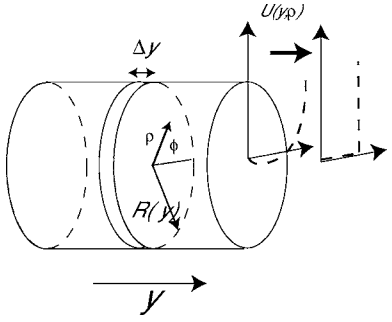

FIG. 2. Geometry along straight channels with parameters defined in the text. Cylindrical symmetry is assumed. Also shown is the abrupt potential approximation used in reducing the more general Eq. (4).

$=n_0(T)\exp[-\beta U(y,\rho)]$, where the integration constant $n_0(T)$ can depend on temperature. Integrating over angle ϕ and the radial coordinate ρ indicated in Fig. 2 and assuming that the effective section of the channel changes negligibly within Δy, the number of particles within a slice Δy along the y direction is

$$\frac{N(y)}{\Delta y} = 2\pi n_0(T) \int_0^{R(y)} e^{-U(y,\rho)/k_B T} \rho d\rho, \tag{3}$$

where $R(y)$ is the cutoff radius of the channel at position y. Beyond such radius it is assumed the potential is sufficiently high that particles will not penetrate within a reasonable temperature range, i.e., break through the pore walls.

Identifying the thermal average lateral position of the particle as $\langle\rho\rangle$, and the lateral partition function as $[1/R(y)]\int_0^{R(y)} \exp[-\beta U(y,\rho)]d\rho = \mathcal{Z}_\perp^{(0)}(y) = e^{-\beta F_\perp^{(0)}(y)}$ we arrive at the expression

$$\frac{N(y)}{\Delta y} = n_0(T) A_0 e^{-\beta F_\perp^{(0)}(y) - k_B T \ln[2\pi\langle\rho\rangle R(y)/A_0]}, \tag{4}$$

where $F_\perp^{(0)}(y)$ is a reference transverse free energy and the logarithmic term is a tranverse entropy term due to the cross section available at a fixed y along the channel. The reference area A_0 is taken to be the diffusive particle excluded volume (in this case the cross section of a methane unit).

A simple limit case that will apply to silicalite is that of an abrupt lateral potential (see Fig. 2), where, as measured from the channel center, it is essentially constant as a function of ρ for a particular value of y and then increases steeply at $R(y)$. Then $F_\perp^{(0)} \sim U(y)$ and $\langle\rho\rangle = R(y)/2$. Now $\pi R^2(y) = A(y)$ is the cross sectional area of the channel. Finally, identifying $k_B \ln[A(y)/A_0]$ as a transverse entropy $S_\perp(y)$, one obtains

$$\frac{N(y)}{\Delta y} = n_0(T) A_0 e^{S_\perp(y)/k_B} e^{-U(y)/k_B T}. \tag{5}$$

The transverse entropy for spherically symmetric particles is related to the logarithm of the transverse area available to them within the channel for a given potential at the same coordinate. This form of the concentration of particles is very useful for MD because one can assess entropic and energetic effects from the density profiles obtained in the simulation. Furthermore, as potential profiles can be obtained independently by a "simulated molecular probe" one can extract the entropic contribution directly.

Equation (5) can be further exploited to obtain, within transition state theory premises [13], the self-diffusivities expressed as $D_s = k_{\text{hop}} a^2$, where k_{hop} is a site-to-site rate constant and a is an average site-to-site distance. One can then express k_{hop} as

$$k_{\text{hop}} = \left[\frac{\omega(T)}{2\pi} e^{S(y^*,T)/k_B} \right] e^{-U(y^*)/k_B T}, \tag{6}$$

where $\omega(T)$ is the temperature-dependent initial site vibrational frequency, $S(y^*)$ is the lateral entropy of the transition state coordinate (at y^*), and $U(y*)$ is the activation energy or the energy cost to put the molecule over the energy barrier for a diffusion step to occur. Obviously, the exponent in the latter equation can be written in terms of $\Delta F(T)$ the activation Helmholtz free energy. When the change in the energy is dominant in a transition, the temperature dependence of the diffusion coefficient reveals an Arrhenius type exponential behavior from which relevant potential barriers can be identified. The prefactor in Eq. (6), in this case, has only a weak temperature dependence. Such a prefactor can nevertheless become dominant and nontrivial entropy dominated temperature effects ensue as the accessible space of the channel changes at a particular temperature. Particularly extreme effects can occur, such as that reported in Ref. [1], where in Linde type-A zeolite, diffusion of ethane can actually be reduced with temperature in the low loading regime because of an increased accessible cage volume and reduced hindrance to rotations.

In this paper we report that nontrivial free energy effects can occur for methane molecules within silicalite zeolites. The interplay between energy cost and available space, or entropy, within the zeolite channels can change as a function of temperature. Such interplay results in a change in preference from channels at lower temperatures to intersections at higher temperature. Such entropic effects result in non-Arrhenius diffusion dependence on temperature that should be accessible to experiments.

IV. DIFFUSION ANISOTROPY AND TEMPERATURE DEPENDENCE

Using MD, diffusion within silicalite in the three axes was monitored (see Fig. 1 for axis convention, where the straight channels are along the y direction). The diffusivities in the three axes can be obtained from the relation $D_x = \langle x(t)^2\rangle/2t$, where $\langle x(t)^2\rangle$ is the mean square displacement, and the corresponding equations for the y and z axes. As discussed before, no interactions are considered between the methane units so we are at the limit of low loading.

Two hundred methane units were simultaneously evolved in time according to the potentials described above within a canonical simulation where the temperature is held constant by the methods described above [14]. The methane units employed do not interact so they are 200 simultaneous realizations of a single methane molecule that in two unit cells

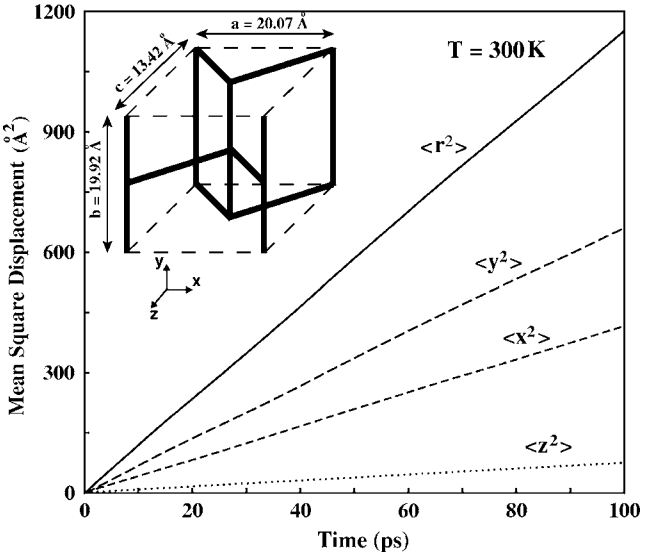

FIG. 3. The mean square displacement as a function of time for the three main axes of silicalite. The axis convention and dimension of the unit cell are shown in the inset. The diffusion coefficient is given by $D=(D_x+D_y+D_z)/3$.

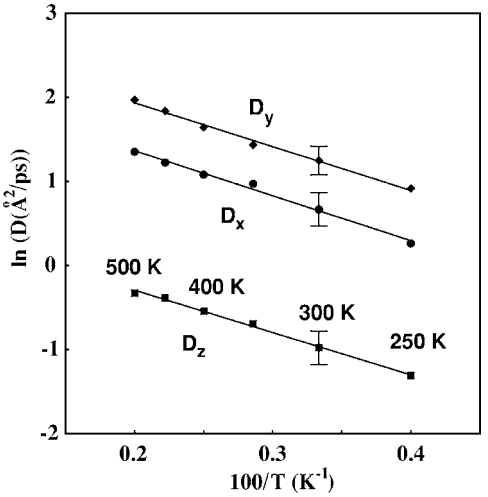

FIG. 4. The diffusivities for the three axes as a function of the inverse temperature in the high-temperature range. As temperature changes diffusion anisotropy is constant within error bars (shown for a single temperature as reference). The three directions obey an Arrhenius type temperature dependence within the shown temperature range.

appropriately describe the dilute limit. The simulation was run for a sufficiently long time, typically 10 ns, such that the concentration profiles within the whole two unit cells no longer changed in time to within 5%. From this point on, we monitored diffusion, computing the diffusitivity in the three axes separately and increasing times as the temperature is lowered using the criterion described in the previous section.

Figure 3 shows the mean square displacement as a function of the simulation time. As expected, the straight channel (along the y) has the largest diffusion coefficient while the diffusion along the z axis, being the combination of diffusion in the x and the y axis, the slowest. The diffusion coefficients obtained are very similar to those of Refs. [10,11,15,16] and are close to those found experimentally in the low loading regime [17]. The diffused distances in the figure allow the conclusion that methane can effectively cover a few silicalite unit cells within the simulation time and that no transient effects are dominating the computations. Diffusion in the x axis is slower than along the straight channel presumably because of the zigzag nature of the channels.

In Fig. 4 we show the diffusivities, for the higher temperature range of our simulations, as a function of the inverse temperature and for the three axes. The temperature dependence is of the Arrhenius type (energy barrier dominated diffusion) and the anisotropy of diffusion is independent of temperature, in that temperature range, within the error bars. That the ratio D_y/D_x is independent of temperature is nontrivial, since the access to intersections from the straight and zigzag channel need not have the same energy barriers. The results seem to suggest a close similarity between transition states of the straight and zigzag channels.

The relative values of the diffusion coefficients in different directions can be assessed by using a relation proposed by Karger [18]. Assuming that diffusion proceeds between an intersection and the next independent of its previous history, on the basis of purely probabilistic considerations, the relation between diffusion constants should be $c^2/D_z=a^2/D_x+b^2/D_y$, where a, b, c are the characteristic lengths of a unit cell of silicalite (see inset of Fig. 3). As one can directly compute diffusivities in each direction, we have verified that such a relation does not hold, meaning that memory effects are involved in diffusion. One can construct a test for such a relation, following Fritzsche and Karger [7] by defining the ratio

$$\beta=\frac{c^2/D_z}{a^2/D_x+b^2/D_y}. \tag{7}$$

Absence of memory effects correspond to the limit $\beta=1$ and deviations thereof reveal history dependences of the way methane goes from one intersection to the next. Our results give a value of $\beta\sim 1.3-1.5$ as measured in the range above 200 K, indicating, according to Ref. [7], that methane "remembers" in which direction it is traveling when it reaches an intersection. This is because of two effects. (i) The probabilities for it to proceed in the same direction as it came into the intersection $p_{x,x}$ (straight) and $p_{y,y}$ (zigzag), and to proceed in the opposite direction $p_{x,-x}$ and $p_{y,-y}$ respectively, differ. In fact, the probabilities to rebound $p_{x,-x}$ ($p_{y,-y}$) are larger than those to proceed in the same direction $p_{x,x}$ ($p_{y,y}$) as a natural consequence of the presence of an obstacle (the intersection). This effect is particular to the silicalite system where the barrier to diffuse into an intersection is larger than that to diffuse along a particular channel. (ii) The probabilities for the particle to change pore channels $2p_{x,y}$ versus stay within a given pore $p_{x,x}+p_{x,-x}$ also differ. Both Ref. [7] and our simulations show that $2p_{x,y}<p_{x,x}+p_{x,-x}$, i.e., the probability to stay within the same pore system is the largest. In the case where no memory effects are present, the quantities compared above would all be equal resulting in a value of $\beta=1$. Of the two effects above, the probability to stay within

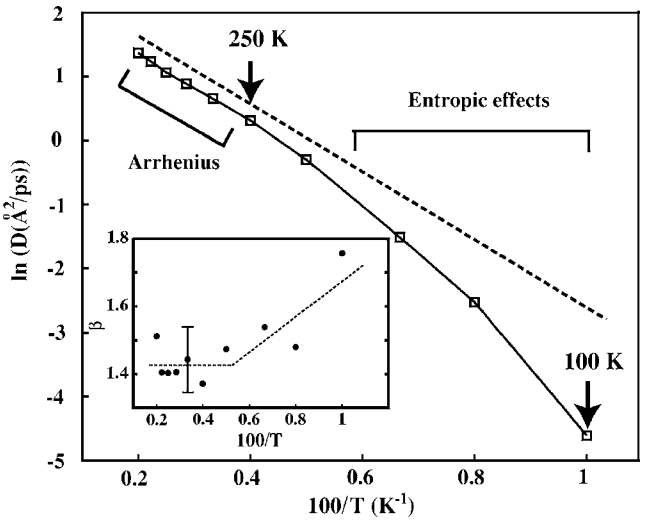

FIG. 5. Crossover to non-Arrhenius-type behavior below ~250 K. The dashed line is a fit to the higher-temperature exponential behavior. In this region entropic effects due to changes in accessible volume as a function of temperature dominate the purely exponential behavior. The inset depicts the memory parameter β which is greater than one in all the temperature range, but increases below 250 K, as explained in the text. The dashed line in the inset is a guide to the eye.

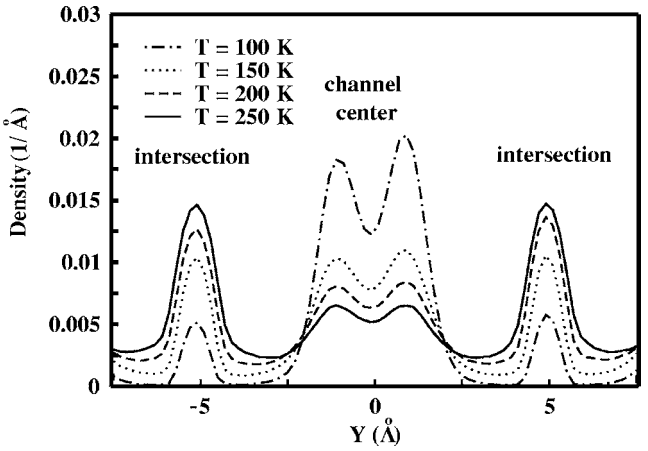

FIG. 6. Density histogram as a function of the y coordinate along the straight channel of silicalite for different temperatures. As temperature is lowered from 250 K the preference for the intersections (indicated $y=\pm 5$ Å) is changed to a preference for the channel centers (indicated in the figure at $y=0$ Å). The temperature at which this crossover occurs is 150 K.

a particular pore is the β increasing (memory increasing) term according to the theory. This is because the fact that $p_{x,-x}$ ($p_{y,-y}$) is larger than $p_{x,x}$ ($p_{y,y}$) actually tends to reduce β towards one reducing memory effects [7].

Fritzsche and Karger also find that as the radius of the intersection decreases, the memory effect is enhanced. This seems intuitive, since large intersection regions prolong particle residence times and will tend to scramble the memory of the jump that placed the particle there (due to multiple collisions or thermal jittering). This is also consistent with the conclusion of those authors that for small intersections, the particles can hop across undetected, presumably meaning that they can continue in the same direction directly jumping beyond the intersection spending very little time at the intersection.

Below 250 K, diffusion goes into a nonArrhenius regime. As shown in Fig. 5 nonexponential behavior dominates (deviations from the dashed line fit to the higher temperature behavior) in such a temperature range suggesting that additional temperature dependences are forthcoming from terms other than purely energetic in nature, namely entropic effects. For quasispherical molecules such as methane, such entropic effects are essentially dependent on the effective available volume as a function of temperature, i.e., as temperature increases, the molecules are able to explore larger regions within the channel structure. This will be discussed through density histograms in the next section.

Diffusion memory changes, below 250 K, are especially revealing. The inset of Fig. 5 shows a systematic increase of memory effects as temperature decreases, while above 250 K they are constant within error bars (only one error bar is shown for reference). As we will see in the next section, this is expected on kinetic grounds since, as temperature is reduced, methane will spend a shorter time at intersections, due to unfavorable energetics, thus preserving memory of the incoming direction in accordance with the arguments given above.

V. PARTICLE DENSITY HISTOGRAMS AND FREE ENERGIES

On the basis of Eq. (5), one can assess both energy and entropic effects from density profiles of methane within the porous structure of the silicalite. We again emphasize that the methane units do not interact so the particles behave as in an ideal gas. The density is then a measure of the probability for particles to occupy a certain position within silicalite. Density histograms were built by performing a simulation of N independent particles, and observing how many of those particles are located within a fixed slice along the y direction in the straight channel. The density is then the number of particles within that slice as implied by Eq. (5). Histograms reach a stationary state where no appreciable changes occurred during simulation time. Figure 6 shows the methane density found in different regions along the y axis in the straight channel. The different channel regions are indicated. As temperature is increased from 100 K, the preferential presence of methane at the channel centers changes to favor the intersections at 250 K. Above such temperature, the intersections continue to be favored as far as 500 K.

According to Fig. 5, the diffusion coefficient at 100 K is of the order of 0.011 Å^2/ps more than three hundred times slower than at 500 K. In order to check that no transient effects are affecting the results at low temperatures one can estimate how effectively methane is visiting the unit cell within the simulated times, of 10 ns for relaxation and 10 ns for the production stage, at this temperature. Using the measured diffusion coefficient one would typically need of the order of 400 ps to diffuse 5 Å. This means methane can cover at least 25 times this distance during the relaxation

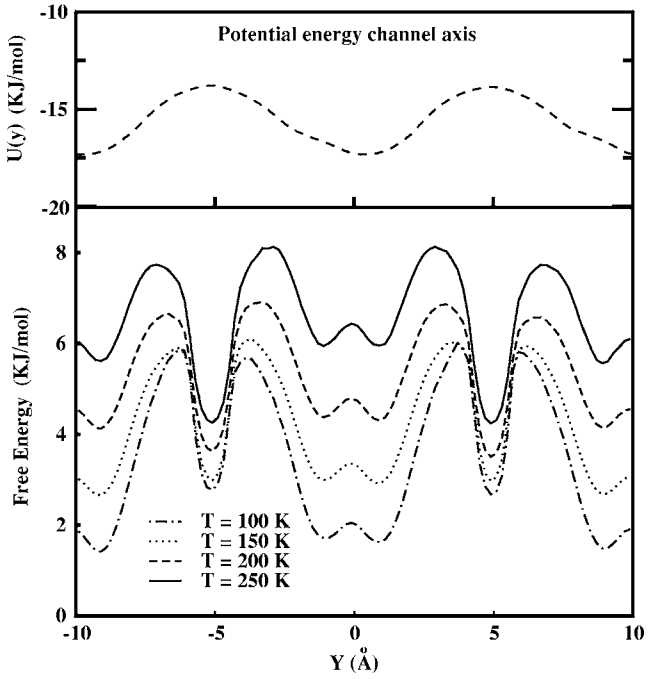

FIG. 7. Local free energy as a function of the y coordinate along the straight channel. The figure is obtained from data of Fig. 5 and the average potential energy, as computed from the simulations at a particular temperature, by using Eq. (5).

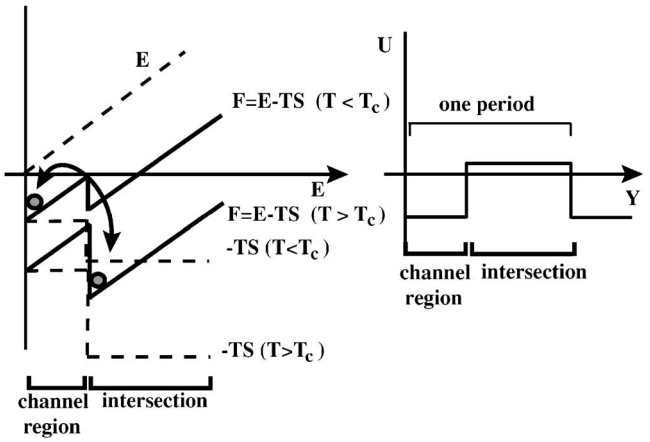

FIG. 8. Global free energy scenario for the first order transition of methane in silicalite. The dashed lines correspond to the energy E and the entropy $\times$ temperature $-TS$. The latter correspond to the available volumes, within the channel region and the intersection region, above ($T>T_c$) and below ($T<T_c$) where T_c is the transition temperature. The continuous lines correspond to the free energy $E-TS$, that exhibit a local and a global minimum. The global minimum dictates methane's spatial preference.

time. We have determined that this is sufficient to reach time independent behavior by fixing temperature at 100 K and starting out from nonequilibrium density distribution. One always reached the final density diagram observed in Fig. 6. The situation does not change by extending simulation times to 20 ns. We thus conclude no transient behavior is involved in the density profiles derived or in the non-Arrhenius behavior regime in Fig. 5.

Changes to a non-Arrhenius behavior in the diffusion depicted in Fig. 5 are then concomitant with change in methane density throughout silicalite. In this temperature range entropic (available volume for spherically symmetric molecules) and purely energetic effects are competing. The potential energy profile at the center of the straight channels, depicted in the top panel of Fig. 7 as reference, shows that it is energetically unfavorable for methane to be at intersections. Nevertheless, the presence there is favored at sufficiently high temperatures. Using Eq. (5) one can derive the local free energy density histogram, to within a constant, directly from the density histogram, as a function of temperature and position y along the straight channel. The result is depicted in Fig. 7, from which essentially the same previous conclusions can be drawn, i.e., lower free energy densities are seen at the channel centers at low temperatures, while this situation changes to favor lower free energies at the intersections at higher temperatures.

As previously mentioned, the average potential energy has lower values in the channel region than it has in the intersections. Notwithstanding, the intersections have a larger lateral dimension per unit length (see qualitative picture in Fig. 1). For a spherically symmetric molecule such as methane, this only means more available volume and thus entropy to any fixed energy. Furthermore, as temperature increases the molecules can further penetrate the potential barrier increasing the available volume until it outweighs the energy handicap. This reasoning applies, in the same way, when comparing densities of methane in the intersection region with those of the zig-zag channels. Thus, while all the following results and discusion will mostly involve the straight channel, diffusion takes place also in the x direction, and the resulting densities at the intersections reflect this fact.

To set up the scenario for the crossover between preferences to the channel center versus intersections one can approach the problem from a complementary microcanonical point of view. One now defines a bulk entropy as a function of the internal energy E by using the relation $S(E) = k_B \ln[V(E)/V_{\text{met}}]$, where $V(E)$ is the accesible volume at energy E and V_{met} is the excluded volume of methane. In Fig. 8 we schematically depict the two contributions to the free energy, namely, the internal energy E and $-TS(E)$ as a function of the internal energy (both are represented by dashed lines). Obviously the internal energy is a linearly increasing function, and the $-TS(E)$ corresponds to the available volume as a function of energy, assuming abrupt potential barriers as shown in the panel on the right (one period, i.e., a complete channel region and one intersection). The importance of the entropic term is weighed by the temperature, so we show two different temperatures $T>T_c$ and $T<T_c$, where T_c is a threshold temperature, to demonstrate the change in the free energy minimum as the entropy associated with volume available in the intersections outweigh their higher energy cost.

According to the previous reasoning; as the average internal energy increases (with temperature) the space accessible to the molecule becomes larger, as molecules further penetrate the potential barriers. At low temperatures, methane is

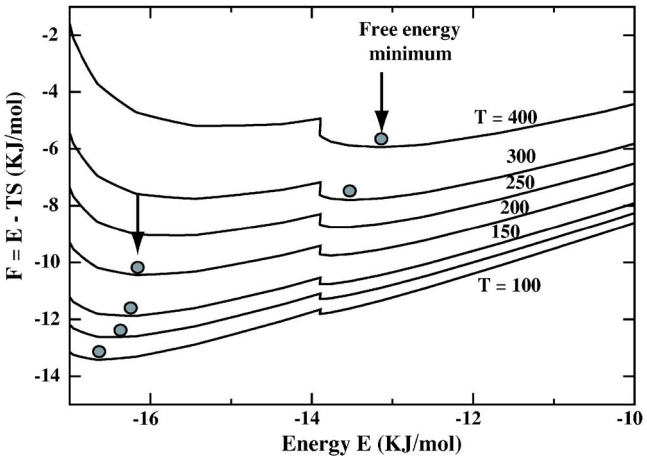

FIG. 9. (Color online) Free energy obtained from estimating volumes within the silicalite potential at a particular available energy. The volumes are determined by the condition $U(r)=E$, where $U(r)$ is the methane-silicalite potential energy. The filled circle indicates the position of the free energy minimum.

confined to the center of the straight channel (or zig-zag channel) where the energy is lower, so according to Fig. 8 the minimum of the free energy density is where the energy is lowest (see grey particle position in figure). As the temperature increases, the space becomes more readily available in spite of the additional energy cost, since there is a large entropy benefit. This new situation redistributes methane's density along the channels, such that the density can be higher at the intersections because of their larger lateral area per unit length.

In order to quantitatively undertake the previous scheme we directly measured the accessible volumes inside the silicalite structure for the straight channels along the y direction, as a function of energy E. The accessible space within the channel region was approximated by a cylindrical region, whose radius r is the perpendicular distance, from the axis, where the potential energy $U(r)$ is the target energy E. This is the maximum classical penetration of the center-of-mass of a methane molecule. Along the channel, the limits of the cylinder are the positions of the transition states y^*. As the distance to the point where $U(r)=E$ is not uniform along the cylinder, the average distance was taken as its radius. Within the intersection region, the space was approximated by a sphere whose radius r is also set by the condition that the potential $U(r)=E$. Nonuniformities were also averaged to yield an effective radius of the sphere. Changes in the details of the procedure for measuring the internal volumes are expected to shift the position of the transition but will yield the same picture.

Figure 9 shows the results for this exercise. Similar conclusions are drawn to those from Fig. 8, making possible a determination of the critical temperature at which the transition occurs, i.e., in between 150 and 200 K. Nevertheless, in these volume assessments of silicalite, we have taken into account volume changes with temperature that were not described by the rough model of Fig. 8. Accurate determination of this threshold temperature is obviously dependent on a precise estimation of the available volume. In the chosen scheme the volume is actually overestimated, since the channel region is not cylindrical as can be assessed from Fig. 6. This results in an overestimation of the threshold temperature.

It is important to note that in the previous calculation we have only included the contribution from the straight pores. The zigzag pore system will evidently have a smaller volume and will thus result in a second critical temperature that will be lower than that of the straight pores. This will broaden the observed transition as the changes in preference towards intersections will occur at different neighboring temperatures.

When the temperature increases beyond 250 K, the increase of available volume as a function of energy decreases sharply as the hard core of the zeolite wall is approached. This leads to a saturation of the entropy effect beyond 250 K (the accessible volume increases very little per unit energy increase). At this point the only temperature dependence is that of potential energy barriers, leading to an exponential temperature dependence. This is the classical Arrhenius type behavior observed in Fig. 5 dominating diffusion beyond 250 K. Evidently, there is now an entropic prefactor determining the magnitude of the diffusion coefficient.

As we mentioned in the previous section on diffusion, there is a close connection between the change in preference towards intersections as temperature increases and memory effects. In the lower temperature regime (<200 K) particles prefer the channel centers strongly, making jumps across intersections a difficult and brief event, because of its energetic handicap. This fact has the tendency to preserve memory of the incoming direction, and reduces the probability for the change of pore systems. This argument is consistent with the tendency of the anisotropy β to increase (see inset of Fig. 5). As temperature increases, the intersections are entropically preferred and methane spends more time at intersections, which tends to reduce memory, although surprisingly β stays at values higher than one. Memory effects are thus present in the whole temperature range studied.

We have performed residence time computations for the intersections, in order to preliminarily determine why memory effects are not reduced further at higher temperatures. We find that in the interval between 200 and 350 K the residence time is essentially the same leading to the conclusion that such a time scale saturates in the high temperature range. The saturation of the residence time according to the arguments given above also limits memory loss and thus the behavior of the anisotropy parameter β follows. This saturation time is surely some compromise between preference to intersections and the tendency to diffuse out of them. Further work on this interesting interplay is forthcoming.

VI. SUMMARY AND DISCUSSION

Summarizing we have reported MD simulations of methane within silicalite in the dilute limit. Computing the diffusion coefficient in the three axes shows the expected anisotropy where the y, straight channels have the largest diffusion coefficient while diffusion in the z direction is the slowest. The high-temperature behavior (300–500 K) is of the Arrhenius type and of diffusion anisotropy independent of temperature within error bars.

Gaining from the probability arguments by Karger *et al.* [7,18], we conclude on the basis of our results, that diffusion shows strong memory effects. This memory is most clearly implied by a tendency to stay within a particular pore due to correlation between the incoming and outgoing direction at an intersection. From the results, it is clear that memory of the incoming direction is not lost and methane has a tendency to continue in the same pore as it came into the intersection. We have shown that memory effects increase as temperature is lowered and residence times, of methane at intersections, decrease. Short residence times avoid memory scrambling at intersections and thus preserve the memory of the incoming direction.

Below 250 K the temperature dependence is no longer Arrhenius, revealing another source of temperature dependence in addition to Boltzmann factors due to energy barriers. Entropic effects were explored by computing the density histograms within the straight channels. We find a change in preference between the channels and intersections below approximately 200 K. Using arguments following from the equality of the chemical potential at equilibrium we derived the local free energy density. A quantitative scenario is proposed, accounting for the change of preference as a function of temperature depending of the volume availabilities in the channel versus the intersection regions.

We have disregarded the effects of the flexibility of the silicalite structure, i.e., vibrations of the confining space. We have already discussed that recent studies of such effects enhance diffusion at room temperature but the effects are uniform in the three spatial direction rendering diffusion anisotropy unaffected. This is consistent with our results by thermalizing through a velocity rescaling mechanism that substitutes physical thermalization by way of collisions to vibrating silicalite pore walls. Differences in the two thermal mechanisms is a very important question regarding the proposed scenario for memory effects. This will depend on how excited modes at a particular temperature deform intersection and channel volumes and the bottle necks that couple them. Within a harmonic aproximation, there should be no dilatation, so no changes in the relative volumes should occur on average. Nevertheless, differential amplitude of vibration between bottlenecks (transition states for jumps between channels and intersections) may influence anisotropy. On the other hand, as temperature is lowered lattice vibrations are less important while memory effects become enhanced, so the picture drawn from our results should be all the more accurate.

The non-Arrhenius behavior of the diffusion coefficient and the regime where entropic effects are strongly temperature dependent are concurrent, the latter serving then as the source of the former behavior. Thus non-Arrhenius behavior in diffusion can be a tell-tale sign of the importance of entropic effects, which although comparatively simple for methane in silicalite, can be very interesting as one studies longer or closed chains (e.g., ethane and benzene). For such systems, entropic effects associated with rotations, and steric restrictions of these degrees of freedom can lead to very nontrivial temperature dependences. The entropic effects observed here are expected to appear in pores systems where there is competition between different pore regions of varying energy costs. In silicalite this occurs between intersection and channel regions. For larger molecules either linear or branched the pore spaces can offer geometric entropic benefits beyond mere volume constraints. Permitting a molecule to rotate or vibrate in particular ways could make an energetically disfavorable region actually beneficial from the free energy point of view, triggering similar transitions. This might also be the case in pore space where stacking efficiency is greater for molecules of a certain shape [3]. Finally, monitoring diffusion anisotropy is also an important sign of both memory and entropic effects, since remanence at intersection regions (controlling memory effects) depends on the entropic benefit of these.

ACKNOWLEDGMENTS

We would like to thank Luis Javier Alvarez for illuminating discussions. This project was funded by Fonacit through Project No. G-97000667.

[1] A. Shuring, S. M. Auerbach, S. Fritzche, and R. Haberlandt, J. Chem. Phys. **116**, 10890 (2002).
[2] R. Krishna, B. Smit, and S. Calero, Chem. Soc. Rev. **31**, 185 (2002).
[3] M. Schenk, S. Calero, Th. Maesen, T. J. H. Vlugt, L. van Benthem, M. Verbeek, B. Schnell, and B. Smit, J. Catal. **214**, 88 (2003).
[4] Z. Lai, G. Bonilla, I. Díaz, J. G. Nery, K. Sujaoti, M. A. Amat, E. Kokkoli, O. Terasaki, R. W. Thompson, M. Tsapatsis, and D. G. Vlachos, Science **300**, 456 (2003).
[5] J. Karger, S. Vasenkov, and S. M. Auerbach, in *Handbook of Zeolite Science and Technology*, edited by S. M. Auerbach, K. A. Carrado, and P. K. Dutta (Marcel Dekker, New York, 2003), pp. 341–422; S. M. Auerbach, F. Jousse, and D. Vercauteren, *Dynamics of Sorbed Molecules in Zeolites, Computer Modelling of Microporous and Mesoporous Materials* (Elsevier, Amsterdam, 2004), pp. 49–108.
[6] F. Jousse, S. M. Auerbach, and D. P. Vercauteren, J. Chem. Phys. **112**, 1531 (2000).
[7] F. Fritzsche and J. Karger, Europhys. Lett. **63**, 465 (2003).
[8] S. Fritzsche, M. Wolfsberg, and R. Haberlandt, Chem. Phys. **289**, 321 (2003).
[9] F. Leroy, B. Rousseau, and A. H. Fuchs, Phys. Chem. Chem. Phys. **6**, 775 (2004).
[10] R. L. June, A. T. Bell, and D. N. Theodorou, J. Phys. Chem. **94**, 8232 (1990).
[11] J. B. Nicholas, F. R. Trow, J. E. Mertz, L. E. Iton, and A. J. Hopfinger, J. Phys. Chem. **97**, 4149 (1993).
[12] S. Fritzsche, M. Wolfsberg, and R. Haberlandt, Chem. Phys. **253**, 283 (2000).
[13] S. M. Auerbach, Int. Rev. Phys. Chem. **19**, 155 (2000).
[14] D. C. Rapaport, *The Art of Molecular Simulation* (Cambridge

University Press, Cambridge, 2004).
[15] P. Demontis, G. B. Suffritti, E. S. Fois, and S. Quartieri, J. Phys. Chem. **94**, 4329 (1990).
[16] S. J. Goodbody, K. Watanabe, and D. MacGowan, J. Chem. Soc., Faraday Trans. **87**, 1951 (1991).
[17] J. Caro, M. Bullow, W. Schirmer, J. Karger, W. Heink, H. Pfeifer, and S. P. Zdanov, J. Chem. Soc., Faraday Trans. **81**, 2541 (1985); W. Heink, J. Karger, and H. Pfeifer, J. Chem. Soc., Faraday Trans. **88**, 3505 (1992).
[18] J. Karger, J. Phys. Chem. **95**, 5558 (1991).